Published in final edited form as:
Mol Pharm. 2009 ; 6(2): 337–344. doi:10.1021/mp800239p.

Nuclear Localization of Cell-Penetrating Peptides is Dependent on Endocytosis Rather Than Cytosolic Delivery in CHO Cells

Jennica L. Zaro, **Jacqueline E. Vekich**, **Thuy Tran**, and **Wei-Chiang Shen***
University of Southern California, School of Pharmacy, Department of Pharmaceutical Sciences, 1985 Zonal Avenue, PSC 404B, Los Angeles, California 90033-1039

Abstract

The nuclear localization of various cell penetrating peptides (CPPs), including Tat [47–57], $YG(R)_9$, $YG(K)_9$, and Model Amphipathic Peptide (MAP), was examined and correlated with the endocytosis and cytosolic transfer efficiency in CHO cells. The results showed that the internalization of the amphipathic peptide, MAP, was much higher than the other cationic CPPs tested. During subcellular fractionation analysis, MAP was only found in the vesicular fraction and was not detectable in the cytosol, similar to the intracellular localization of $YG(K)_9$ as previously determined. This localization pattern differs greatly from the cationic CPPs oligoarginine and Tat, which were previously found primarily in the cytosol. Both quantitative and qualitative analysis of MAP showed high nuclear localization, with staining in perinuclear vesicles. On the other hand, $YG(R)_9$ was found to be excluded from the nucleus. Lysosomotropic amines altered the nuclear localization of the CPPs tested, and the change was correlated with the release of degradation products from the treated cells. These results suggest that highly endocytosed CPPs such as MAP may be more suitable for nuclear drug delivery applications than peptides such as Tat and $YG(R)_9$ that are efficiently delivered to the cytosol.

Keywords

model amphipathic peptide; nuclear localization; Tat; Cell penetrating eptides; endocytosis

Introduction

Cell-penetrating peptides (CPPs) have been studied extensively as a potential carrier-mediated drug delivery system for bioactive agents with low bioavailability[1, 2]. Although there have been numerous studies on the internalization properties of CPPs, the mechanism has been largely under debate and many conflicting reports have been made depending on the cell type under investigation, the detection method used, and the cargo attached to the CPPs [3]. Also multiple processes of internalization occur concurrently leading to diverse subcellular localization profiles for each CPP, further complicating matters, especially with regard to the quantitation method used to determine internalization. Using a subcellular fractionation method, several CPPs have been analyzed for cytosolic versus vesicular localization[4, 5]. It was found that, in cultured Chinese hamster ovary (CHO) cells, both Tat (47–57) and $YG(R)_9$ were localized primarily in the cytosol, while $YG(K)_9$ was highly endocytosed[4]. However, the two processes of internalization are dependent on minor alteration of the structure of CPPs. For example, the partial guanidination of the ε-amino groups in $YG(K)_9$ showed an increased in the amount internalized into the cytosol, while an

*To whom correspondence should be addressed: Dr. Wei-Chiang Shen, University of Southern California, School of Pharmacy, Department of Pharmacology and Pharmaceutical Sciences, 1985 Zonal Avenue, PSC 404B, Los Angeles, California 90033-1039, Telephone: (323) 442-1902, Fax: (323) 442-1390. weishen@usc.edu.

increase of the size of oligoarginine from $YG(R)_9$ to $YG(R)_{16}$ significantly increased the uptake of oligoarginine by endocytosis[4].

It is commonly thought that CPPs that are internalized into the cytosol of cells would facilitate nuclear transport of conjugated agents. In theory, peptides located in the cytoplasm are more accessible to nuclear trafficking machinery and less likely to be degraded, as opposed to endocytosed peptides that are enclosed in endocytic vesicles and readily trafficked to the lysosome. As a result, many studies focus on CPPs for delivery of agents that require nuclear localization for their bioactivity, for example in gene therapy[6–8], where delivery efficiency is determined by measuring gene expression levels [9]. However, this methodology does not provide conclusive information regarding cytosolic localization since a clear relationship between cytosolic and nuclear transport has not been established. In this report, the nuclear transport of several CPPs, including the model amphipathic peptide (MAP)[10, 11], is correlated with the internalization pathway. While pathways including direct membrane penetration into the cytosol, termed “membrane transduction”, and endocytosis could be useful for drug delivery, each process may be optimal to deliver different types of drugs or deliver drugs to certain targets within the cell.

Experimental Section

Peptide Synthesis and ^{125}I-labeling

Model amphipathic peptide (MAP) (Y-KLALKLALKALKAALKLA), Tat [47–57] (YGRKKRRQRRR), $YG(R)_9$, and $YG(K)_9$ were synthesized using solid phase synthesis by Genemed (San Antonio, TX). A tyrosine moiety was included in all of the peptides to allow for labeling with Na-^{125}I (MP Biomedicals Inc, Irvine, CA) using the Chloramine-T method[12]. The labeled oligopeptides were purified by size exclusion chromatography using a Sephadex G-15 (Amersham Biosciences, Uppsala, Sweden) column, and quantitated using a gamma counter (Packard, Downers Grove, IL).

Cell culture

Both Chinese hamster ovary (CHO) and A431 human epidermoid carcinoma cell lines were obtained from American Type Culture Collection (Manassas, VA). CHO cell monolayers were grown in Ham’s F12/Dubecco’s Minimum Essential Media (DMEM), and A431 cells were grown in DMEM (Mediatech Cellgro, VA). The media for both cell lines was supplemented with 10% (v/v) fetal bovine serum (FBS), (Gemini Bio-Products, Woodland, CA), 1 mM l-glutamine, 50 U/mL penicillin and 50 μg/mL streptomycin (Invitrogen/Gibco, Grand Island, NY). The toxicity following treatment with 5 μg/mL CPPs was determined using the trypan blue assay, where it was determined that cell viability was >95% for all peptides.

Guanidination of MAP

The lysyl ε-amino groups of MAP were guanidinated as previously described[4, 13], and purified using size exclusion chromatography with a Sephadex G-15 column. The fractions containing MAP, as determined by UV Spectroscopy (Bausch & Lomb, Rochester, NY) at 280 nm were pooled and the amount of free lysyl ε-amino groups remaining was determined using the 2,4,6-Trinitrobenzene Sulfonic Acid Assay according to the manufacturer’s instructions (Sigma). The percentage of guanidine modification was estimated using a MAP standard curve, where it was determined that approximately all five (99.7%) of the lysyl groups of MAP were modified.

Subcellular Fractionation

Confluent CHO cell monolayers grown in T-75 tissue culture flasks were pre-incubated with serum-free media for 10 min and subsequently treated with serum-free media containing 5 μg/mL of ^{125}I-labeled peptide, 0.1 mg/mL FITC-Dextran (40 kDa) and a protease inhibitor cocktail (PI) containing 4 μM AEBSF, 2 μM EDTA, 0.3 μM bestatin, 30 nM E-64, 2 μM leupeptin and 0.6 nM aprotinin (Sigma). After a 1 h incubation at 37 °C, cells were processed for the measurement of cytosolic and vesicular amounts as described in previous reports[4, 5].

Confocal Microscopy

MAP and YG(R)$_9$ were labeled with fluorescein by reacting with fluorescein isothiocyanate (FITC). 40 mM FITC (Sigma) was added to a 2 mM peptide solution in a molar ratio of 2:1, and the solution was incubated at 4 °C for 18 h. The free FITC was removed from the reaction mixture by dialysis (1000 MW cutoff, cellulose ester membrane, Spectrum Laboratories, Inc., Rancho Dominguez, CA) against 0.5 M ammonium bicarbonate overnight. The absorbance of the purified reaction mixture at 480 and 280 nm was determined to calculate the FITC/peptide molar ratio, which was approximately 1:1 for both peptides.

To quantitatively evaluate internalization, the CHO cells were grown in poly-D-lysine coated 6-well plates overnight. Dosing solutions of 5 μg/mL FITC-labeled conjugates were incubated in serum containing 5% FBS for 2 h at 37°C. The cell monolayers were rinsed consecutively three times with 3 mL cold PBS, cold heparin-PBS (0.5 mg/mL), and cold PBS, and then replenished with fresh serum-free medium. The live cells were imaged using a Zeiss LSM 510 Meta NLO confocal imaging system.

Nuclear Isolation and Total Internalization

Before peptide treatment of the confluent cell monolayers, media containing FBS was removed and cells were incubated with serum-free media for 30 min at 37 °C, followed by treatment with 5 μg/mL ^{125}I-oligopeptide in serum-free media for the indicated time point. If the cells were to be treated with an endosomal acidification inhibitor, 50 mM NH_4Cl or 200 μM chloroquine (Sigma) were added to the serum-free media and pre-incubated for 30 min followed by incubation with the peptide dosing solution containing the inhibitors for the indicated time period. The labeled cells were washed with cold PBS, detached with trypsin, and centrifuged. After additional washes with heparin-PBS and PBS, the total internalization was determined by measuring the radioactivity of the cell pellet, and the nuclear accumulation was measured as previously described[5, 14].

Peptide Degradation Analysis

Confluent CHO cell monolayers grown in 6-well cluster plates were pre-incubated with serum-free media with and without 50 mM NH_4Cl or 200 μM chloroquine for 30 min and subsequently incubated with 5 μg/mL ^{125}I-labeled peptide in serum-free media for 1 h at 37°C. The dosing media was removed, and the cells were washed thoroughly 3 times each with ice cold 0.5 mg/mL heparin-PBS, followed by washing with ice cold PBS. Subsequently, the cells were replenished with fresh serum-free media. After a 1 h re-incubation at 37 °C, the chase media was removed and the cell monolayers were thoroughly washed, and detached with trypsin-EDTA. The isolated cell pellet was washed, and the cell pellet and chase media were analyzed for radioactivity. Degradation was determined as a percentage of the radioactivity remaining in the cell versus the amount of radioactivity found in the chase media after the 1 hour incubation.

Data Analysis

For the quantitative analyses, the data are presented as average plus standard deviation with n > 3 for all experiments. The Student's t-test was utilized to compare data sets, where values with $p < 0.05$ were considered statistically significant.

Results

Internalization of MAP

The cytosolic versus vesicular localization of internalized MAP was determined in CHO cells. The results show that the internalized MAP was found only in the vesicular compartments, with none of the labeled oligopeptide detectable in the cytosol. After guanidination of the lysyl residues in MAP, the cytosolic amount of the peptide significantly increased from a non-detectable amount to 65% (Table 1).

Nuclear Transport

The nuclear transport of several radiolabeled CPPs including MAP, Tat [47–57], $YG(R)_9$, and $YG(K)_9$ was determined in CHO and in A431 cells. The total internalization of MAP is significantly higher than that of other cell-penetrating peptides (CPPs) such as oligoarginine, oligolysine, and Tat peptide. However, as shown in Table 2, the highly endocytosed CPP, MAP, showed the highest nuclear accumulation. The CPPs that have been previously shown to be internalized efficiently into the cytosol, $YG(R)_9$ and Tat, were found in comparatively lower amounts in the nuclear compartment, while $YG(K)_9$, which was previously shown to be internalized predominantly by endocytosis, had very little nuclear accumulation. The nuclear transport efficiencies were similar in both cell lines, with MAP showing comparatively higher nuclear transport in CHO and in A431 cells.

Kinetics of Nuclear Transport

The nuclear transport of MAP and $YG(R)_9$ was further compared. Figure 1 shows that the nuclear accumulation of MAP does not significantly increase from 1 to 2 hours, revealing that nuclear transport of MAP is relatively fast and levels off after approximately 1 h. In addition, it appears that nuclear transport of MAP occurs immediately after cellular internalization because it has almost no cytosolic localization and high nuclear localization from very early time points. The increase in the amount of MAP accumulated in the nuclear fraction correlates with a decrease in the amount found in the vesicles. This result suggests that the nuclear fraction is not contaminated with membrane bound MAP, since the kinetics of nuclear transport are very different than those for endocytosis, and for the membrane binding amounts (data not shown). Alternatively, $YG(R)_9$ did show a significant increase in nuclear localization over this time frame consistent with previous data [5]. Since nuclear localization of $YG(R)_9$ was approximately 3.5-fold less than MAP, 2 hour time periods were used in the following nuclear localization experiments to increase the measurement accuracy.

Confocal Microscopy

The nuclear accumulation of MAP and $YG(R)_9$ were qualitatively validated using confocal microscopy following a 2 h incubation with 5 μg/mL FITC conjugated peptide (Figure 2). Figure 2A shows that FITC alone distributes evenly throughout all of the cells, represented by the green fluorescence. When cells were incubated with the MAP conjugate, an uneven distribution of the peptide occurs, with marked accumulation of fluorescence inside vesicles in the perinuclear region (Figure 2B), supporting that internalization of MAP is through endocytosis. The fluorescence of the oligoarginine ($YG(R)_9$) conjugate was found diffuse

throughout the cytoplasm with apparent exclusion from the nucleus, with only about 50% of the cells showing fluorescent staining (Figure 2C).

The Effects of Ammonium Chloride

The nuclear transport and total internalization of ^{125}I-labeled MAP, YG(K)$_9$, and YG(R)$_9$ was quantitatively determined following treatment with 50 mM ammonium chloride (NH_4Cl). Ammonium chloride is a lysosomotropic agent, which inhibits endosomal acidification and consequently slows endocytosis. The results showed that treatment with ammonium chloride treatment increases the nuclear localization of MAP and YG(K)$_9$, while treatment slightly decreases the nuclear localization of YG(R)$_9$ (Figure 3). The total internalization of the CPPs tested was not significantly affected by treatment with ammonium chloride.

Chloroquine, a More Potent Lysosomotropic Inhibitor

The nuclear localization and total internalization of MAP, YG(K)$_9$, and YG(R)$_9$ was also examined using chloroquine. Like ammonium chloride, chloroquine is also a lysosomotropic amine and inhibits endosomal acidification by the same mechanism; however, it is a more potent lysosomotropic agent and is also known to be a lysosomal protease inhibitor[15]. Comparable to the results obtained with ammonium chloride, chloroquine increases nuclear localization of MAP and YG(K)$_9$, though to a greater extent. Treatment with chloroquine also increases the nuclear localization YG(R)$_9$, which is in contrast to the results obtained with ammonium chloride (Figure 4A). The total internalization of all three of the peptides tested was also slightly increased (Figure 4B).

Cell-penetrating Peptide Degradation

To evaluate the role of degradation in the effects of the endocytic inhibitors, CHO cells were dosed with ^{125}I-labeled MAP, YG(K)$_9$, or YG(R)$_9$ for 1 hour, the treatment medium was replaced with fresh media after washing the cell monolayer, and degradation was examined over a 1 hour time period. Following intracellular degradation of a ^{125}I-labeled peptide, the iodinated tyrosine residue is excreted into the media since it cannot be recycled for use within the cell[16]. Using this rationale, degradation was measured as a percentage of the radioactivity remaining in the cell versus the radioactivity released into the chase media.

As shown in Figure 5, the amount of MAP remaining in the cell after a 1 hour chase is higher than both YG(K)$_9$ and YG(R)$_9$. In fact, almost all of the YG(K)$_9$ was found in the medium, with very little remaining in the cell after the 1 hour chase period. This may indicate differences in the internalization and processing of the amphipathic versus cationic oligopeptides. The effects of ammonium chloride and chloroquine on the release of ^{125}I-peptides were also evaluated. As shown in Figure 5, both ammonium chloride and chloroquine increased the amount of ^{125}I-labeled MAP and YG(K)$_9$ remaining in the cell (i.e., decreased the release of degraded peptide). Chloroquine had a more significant effect on the retention of the oligopeptide than NH_4Cl did. Alternatively, ammonium chloride and chloroquine had different effects on the degradation of YG(R)$_9$. While ammonium chloride increased the degradation (i.e. decreased the amount remaining in the cell), chloroquine decreased the degradation, similar to MAP and YG(K)$_9$.

Discussion

It is generally thought that the amphipathic and the cationic CPPs may not share common internalization pathways[1]. To further evaluate the intracellular localization of the amphipathic peptide, MAP, the cytosolic versus vesicular localization was determined using subcellular fractionation[4]. The data showed that the internalization of MAP was high in

comparison to other common CPPs, including oligoarginine, oligolysine, and Tat, however it was localized only in the vesicular fraction in CHO cells. The sequence of MAP only contains cationic lysine residues, not arginine. Since the guanidine moiety of arginine has been implicated to facilitate membrane transduction due to the bidentate bonds it forms with the anionic cell surface[4, 17], the lysyl groups were N-guanidinated, which led to an increase in the amount of MAP in the cytosolic fraction. Consistent with previous results, this data indicates that while the simple charge interaction of the lysyl ε-amino group with anionic groups on the cell surface is sufficient for endocytosis, the guanidine moiety is important for cytosolic transfer[4]. Interestingly, the guanidination significantly decreased the total amount of MAP internalized. This result is consistent with a study where it was shown that the biological activity of a peptide nucleic acid conjugated to a MAP-derivative with lysine to arginine substitutions, RLALRLALRALRAALRLA, was lower than the activity obtained when conjugated to MAP [18]. The decrease in overall internalization could be due to an alteration in the alpha-helical structure of MAP, which contributes greatly to the internalization of the CPP [11, 19].

During subcellular fractionation analysis, it was observed that the post-nuclear pellet, which contains cell nuclei as well as other membrane debris, contains a high amount of MAP. Therefore, the nuclear localization of MAP was further evaluated. Qualitative analysis of nuclear localization using confocal microscopy showed that MAP is localized in the nucleus and has an increased staining in intracellular vesicles which appear at the periphery of the nucleus. On the other hand, oligoarginine was found to be excluded from the nucleus. The distribution of $YG(R)_9$ throughout the cytosol appeared as very small specks, which is similar to the distribution seen for cytosolic proteins associated with lipid droplets (LDs) present in the cytoplasm, indicating that CPPs may be associated with these or other cytoplasmic particles in the cytosol[20, 21].

Nuclear transport kinetic studies of the MAP and $YG(R)_9$ peptides reveal two different profiles. While the nuclear accumulation of MAP was high after the 1 h timepoint and leveled off at 2 h, oligoarginine increased only after 1 hour, which is consistent with other reports[5, 22]. Therefore, compared to MAP, the nuclear transport process of $YG(R)_9$ is broken up into two parts, in which the peptide is rapidly internalized into the cytoplasm within 15 min by transduction and is then slowly transported to the nucleus after 1 hour.

MAP was not detected in the cytosol, which could possibly be due to the rapid transit from the cytosolic compartment to the nucleus. However, this pathway seems unlikely for peptides such as MAP that do not contain a classical nuclear localization signal (NLS)[23, 24], where, as previously mentioned, the cytosolic transit is generally slow. Therefore, the abundance of MAP in the nucleus may be due to the higher overall internalization (Figure 4), or the high accumulation near the perinuclear region as seen in Figure 2B. The transport of plasma membrane-bound ligands to the nucleus via endocytosis has been reported for several cytokines and growth factors, and it has been shown that the nuclear transport of these proteins is affected by treatment with lysosomotropic amines [5].

The internalization and nuclear transport of MAP was further evaluated following treatment with lysosomotropic amines including ammonium chloride and chloroquine. While treatment with either ammonium chloride or chloroquine did not significantly alter the total internalization of MAP, the nuclear transport was significantly increased. The lack of effect on the total internalization may be explained by the action of lysosomotropic agents in decreasing endosomal fusion events with the lysosome, and consequently inhibiting lysosomal degradation of the peptides[25]. While the internalization may be decreased, the degradation and release of peptides out of the cell may also be slowed, leaving the total amount of oligopeptide inside the cell unchanged. This speculation is supported by the

observed decrease in the release of MAP degradation products following treatment with ammonium chloride and chloroquine (Figure 5), which suggests a balance between inhibition of uptake and degradation. The inhibition of degradation may also explain the increase in nuclear localization of MAP, since accumulation of peptide in the cell leaves more peptide available to be transported to the nucleus via an unknown mechanism.

The degradation data also showed that, in comparison to MAP, most of the oligolysine is released into the chase media following a 1 h incubation. This data could explain why the nuclear localization and internalization of $YG(K)_9$ is significantly lower than MAP, even though both are internalized primarily by endocytosis. MAP may be innately more resilient against degradation, possibly due to the hydrophobic character. Upon endocytosis MAP may coat or imbed itself into the inner leaflet of the endosomal membrane, making it less accessible to proteases and potentially facilitate its endosomal escape[26].

The internalization and nuclear transport of $YG(R)_9$ following treatment with lysosomotropic amines showed slightly different results. Ammonium chloride treatment slightly decreases nuclear localization the highly transduced peptide $YG(R)_9$, which was expected to remain unaffected since it was previously observed that ammonium chloride had no effect on the nuclear localization of this peptide[5]. Consistent with the slight decrease in nuclear localization, the total internalization of $YG(R)_9$ is also slightly decreased. The slight decrease in nuclear localization could be due to natural variation, or due to the differences in the incubation timepoints. The previous study evaluated the effect of ammonium chloride on nuclear localization at a 1 h timepoint, as opposed to the 2 h timepoint used in this study. Alternatively, chloroquine increased the nuclear accumulation of oligoarginine, similar to MAP and $YG(K)_9$. The effects of ammonium chloride and chloroquine on the nuclear transport of $YG(R)_9$ correlated with degradation, since ammonium chloride increased the release of $YG(R)_9$, while chloroquine increased the retention (Figure 5). The results for oligoarginine are interesting since they show a differential effect of two lysosomotropic amines on the processing of the CPP. It is important to keep in mind that a small fraction of $YG(R)_9$ is internalized by endocytosis, which may be why it is affected by lysosomotropic agents. Since chloroquine is a more potent lysosomotropic agent and has a broader effect on other endocytic processes including lysosomal protease inhibition[15], the decreased degradation may play a role in the increased nuclear transport, similar to MAP and $YG(K)_9$. Chloroquine has also been shown to be an inhibitor of the autophagy pathway[27], which could possibly be involved in the processing of cytosolic oligoarginine. In addition to these pathways, weak bases also have an effect on cytosolic pH[28, 29], which may impact the CPPs with high cytosolic localization. In any case, these data indicate that the effects of the lysosomotropic amines are different for CPPs localized mainly in the cytosol versus endocytic vesicles.

In conclusion, peptides with very little cytosolic localization showed high nuclear transport. Taken together, the data indicate that the nuclear transport follows endocytosis, similar to results seen for many growth factors and cytokines [28, 29]. Therefore, against common beliefs, it appears that highly endocytosed CPPs such as MAP may be more suitable for nuclear drug delivery applications as opposed to some of the highly transduced peptides. However, it should be pointed out that results presented in this report were obtained from the studies of the transport of CPPs alone. Conceivably, depending on the size, charge, method of attachment, and other physicochemical properties of the cargos, the attachment of drug molecules may interfere with the internalization processes of CPPs[1, 3]. Therefore, a careful evaluation of the drug molecule of interest on the internalization and trafficking of CPPs will be required for applying MAP as a nuclear transport carrier in the design of drug delivery systems.

Abbreviations

CPP	Cell Penetrating Peptide
DMEM	Dubecco's Minimum Essential Media
FBS	Fetal bovine serum
MAP	model amphipathic peptide
NH_4Cl	ammonium chloride
PBS	phosphate buffered saline

References

1. Patel LN, Zaro JL, Shen WC. Pharmaceutical Research. 2007; 24:1977–1992. [PubMed: 17443399]
2. Fischer PM. Medicinal Research Reviews. 2007; 27(6):755–795. [PubMed: 17019680]
3. El-Andaloussi S, Jarver P, Johansson HJ, Langel U. Biochemical Journal. 2007; 407:285–292. [PubMed: 17627607]
4. Zaro JL, Shen WC. Biochemical and Biophysical Research Communications. 2003; 307(2):241–247. [PubMed: 12859946]
5. Zaro JL, Shen WC. Experimental Cell Research. 2005; 307(1):164–173. [PubMed: 15922736]
6. Shen WC. Journal of Drug Targeting. 1997; 5(1):11–13. [PubMed: 9524309]
7. Mann A, Thakur G, Shukla V, Ganguli M. Drug Discovery Today. 2008; 13(3–4):152–160. [PubMed: 18275913]
8. Torchilin VP. Annual Review of Biomedical Engineering. 2006; 8:343–375.
9. Tung CH, Weissleder R. Advanced Drug Delivery Reviews. 2003; 55(2):281–294. [PubMed: 12564981]
10. Oehlke J, Scheller A, Wiesner B, Krause E, Beyermann M, Klauschenz E, Melzig M, Bienert M. Biochimica Et Biophysica Acta-Biomembranes. 1998; 1414(1–2):127–139.
11. Scheller A, Oehlke J, Wiesner B, Dathe M, Krause E, Beyermann M, Melzig M, Bienert M. Journal of Peptide Science. 1999; 5(4):185–194. [PubMed: 10323198]
12. Sonoda S, Schlamow M. Immunochemistry. 1970; 7(11):885. [PubMed: 5531224]
13. Beardsley RL, Reilly JP. Analytical Chemistry. 2002; 74(8):1884–1890. [PubMed: 11985322]
14. Beck LA, Hosick TJ, Sinensky M. Journal of Cell Biology. 1988; 107(4):1307–1316. [PubMed: 3170631]
15. Wibo M, Poole B. Journal of Cell Biology. 1974; 63(2):430–440. [PubMed: 4607946]
16. Taub ME, Wan JS, Shen WC. Pharmaceutical Research. 1994; 11(9):1250–1256. [PubMed: 7816752]
17. Rothbard JB, Jessop TC, Wender PA. Advanced Drug Delivery Reviews. 2005; 57(4):495–504. [PubMed: 15722160]
18. Wolf Y, Pritz S, Abes S, Bienert M, Lebleu B, Oehlke J. Biochemistry. 2006; 45(50):14944–14954. [PubMed: 17154532]
19. Scheller A, Wiesner B, Melzig M, Bienert M, Oehlke J. European Journal of Biochemistry. 2000; 267(19):6043–6049. [PubMed: 10998065]
20. Ostermeyer AG, Ramcharan LT, Zeng YC, Lunlin DM, Brown DA. Journal of Cell Biology. 2004; 164(1):69–78. [PubMed: 14709541]
21. Targett-Adams P, Chambers D, Gledhill S, Hope RG, Coy JF, Girod A, McLauchlan J. Journal of Biological Chemistry. 2003; 278(18):15998–16007. [PubMed: 12591929]
22. Sandgren S, Cheng F, Belting M. Journal of Biological Chemistry. 2002; 277(41):38877–38883. [PubMed: 12163493]
23. Lange A, Mills RE, Lange CJ, Stewart M, Devine SE, Corbett AH. Journal of Biological Chemistry. 2007; 282(8):5101–5105. [PubMed: 17170104]

24. Fontes MRM, Teh T, Kobe B. Journal of Molecular Biology. 2000; 297(5):1183–1194. [PubMed: 10764582]

25. Seglen PO, Grinde B, Solheim AE. European Journal of Biochemistry. 1979; 95(2):215–225. [PubMed: 456353]

26. De Kroon AIPM, Vogt B, Van'T Hof R, De Kruijff B, De Gier J. Biophysical Journal. 1991; 60(3):525–537. [PubMed: 1932545]

27. Boya P, Gonzalez-Polo RA, Casares N, Perfettini JL, Dessen P, Larochette N, Metivier D, Meley D, Souquere S, Yoshimori T, Pierron G, Codogno P, Kroemer G. Molecular and Cellular Biology. 2005; 25(3):1025–1040. [PubMed: 15657430]

28. Holtzman, E., editor. Lysosomes. Plenum Press; New York: 1989. p. 93-160.

29. Tapper H, Sundler R. Biochemical Journal. 1990; 272(2):407–414. [PubMed: 2268269]

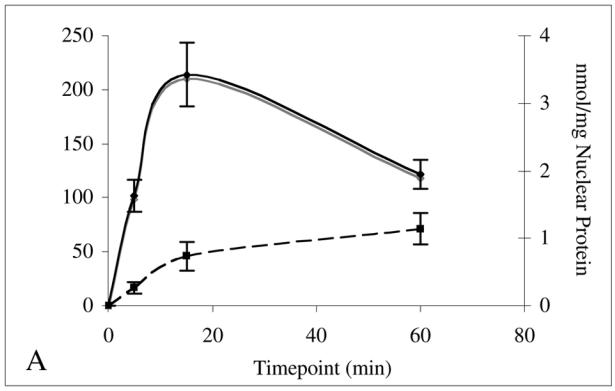

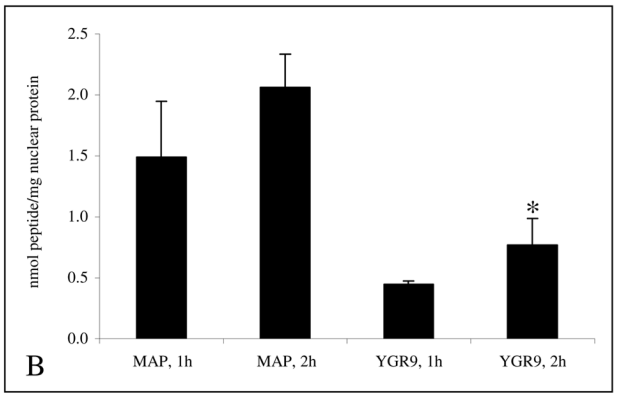

Figure 1.

Nuclear Transport Kinetics. CHO cultured cell monolayers were treated with serum-free medium containing 5 μg/mL ^{125}I-labeled peptides for the indicated time points at 37 °C. (A) The amount of ^{125}I-MAP internalized by endocytosis (solid line, primary axis) and accumulated in the nucleus (dashed line, secondary axis) was determined as described in the Materials and Methods section. Data are represented as the average of duplicate sample measurements and error bars indicate the standard error. (B) Treated cells were detached following incubation with trypsin and the nuclear accumulation was determined as described in the Materials and Methods section. The bars represent the average of triplicate sample measurements, the errors bars represent the standard deviation, and bars marked with an asterisk indicates a statistically significant difference ($p < 0.05$) in results from two different timepoints.

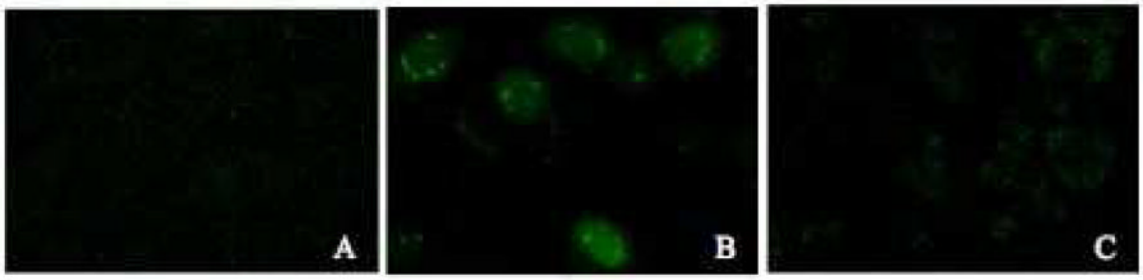

Figure 2.

Localization of FITC-peptide conjugates. Cultured CHO cell monolayers were treated with medium containing 5% FBS and 5 μg/mL (**A**) FITC alone, (**B**) FITC-MAP, or (**C**) FITC-$YG(R)_9$ for 2 hours at 37 °C. Cells were washed with heparin-PBS and PBS, and analyzed by confocal microscopy as described in the Materials and Methods section.

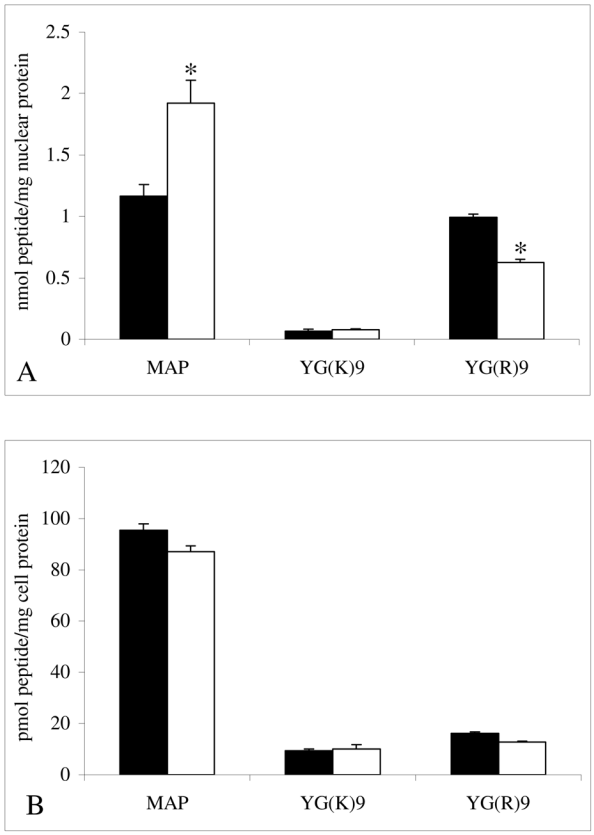

Figure 3.

The Effects of Ammonium Chloride. To determine the effect of ammonium chloride on nuclear transport (Figure A) and total internalization (Figure B), cultured CHO cell monolayers were treated with serum-free medium containing 5 μg/mL ^{125}I-labeled peptide for 2 hours at 37 °C in the absence (solid bars) and presence (open bars) of 50 mM NH_4Cl. The nuclear and total intracellular accumulation was determined as described in the Material and Methods section. The bars represent the average of triplicate sample measurements, the errors bars are the standard deviation, and bars marked with an asterisk indicates a statistically significant difference ($p < 0.05$) in comparison to results obtained from the non-treated (control) cells.

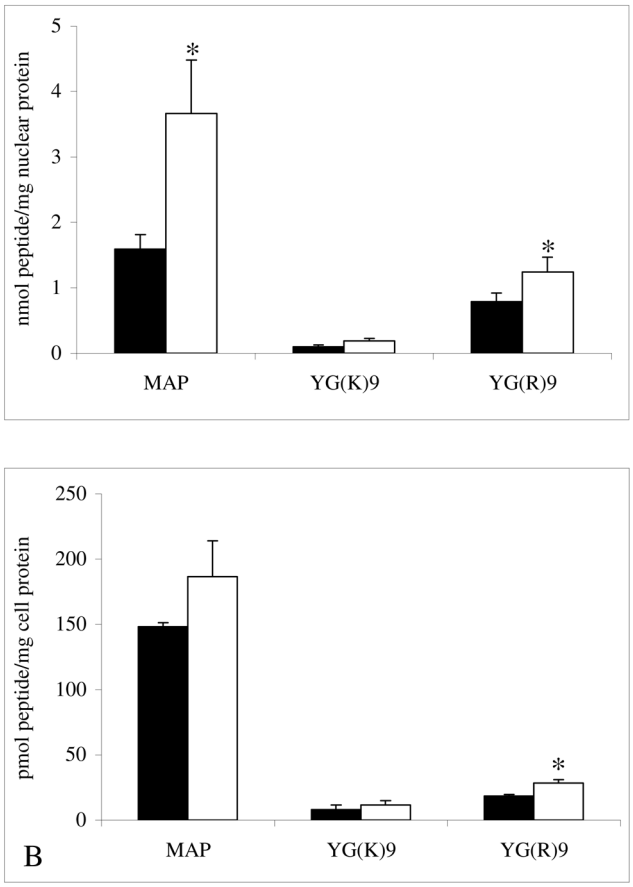

Figure 4.

The Effects of Chloroquine. To determine the effect of chloroquine on nuclear transport (Figure A) and total internalization (Figure B), cultured CHO cell monolayers were treated with serum-free medium containing 5 μg/mL ^{125}I-labeled peptide for 2 hours at 37 °C in the absence (closed bars) and presence (open bars) of 200 μM chloroquine. The nuclear and total intracellular accumulation was determined as described in the Material and Methods section. The bars represent the average of triplicate sample measurements, the errors bars are the standard deviation, and bars marked with an asterisk indicates a statistically significant difference ($p < 0.05$) in comparison to results obtained from the non-treated (control) cells.

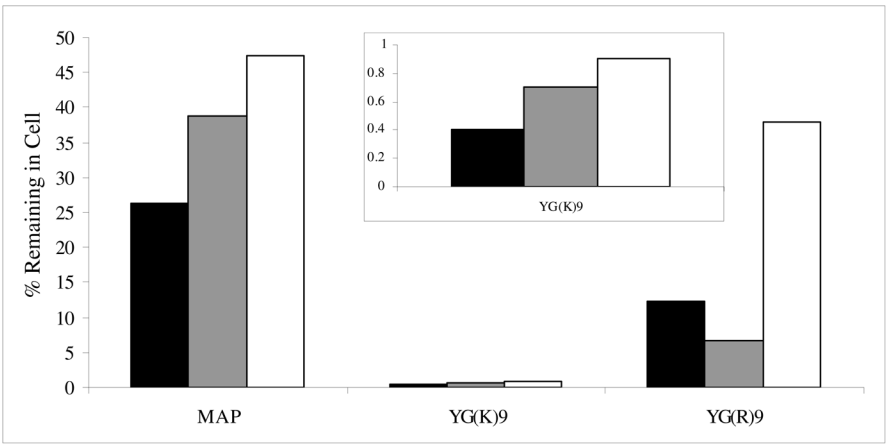

Figure 5.

Release of Degradation Products in CHO cells. To determine the effect of ammonium chloride and chloroquine (CQ) on the release of degradation products following treatment with MAP, $YG(K)_9$, or $YG(R)_9$, cultured CHO cell monolayers were treated with serum-free medium containing 5 μg/mL ^{125}I-labeled peptide for 1 hour at 37 °C in the absence (black bars) or presence of 50 mM NH_4Cl (gray bars) or 200 μM chloroquine (open bars). The cell monolayers were then extensively washed, and fresh serum-free medium in the absence or presence of endocytosis inhibitors was added and the cells were incubated for an additional hour at 37 °C. Data are represented as a % Remaining in Cell ([amount of ^{125}I-labeled peptide released to chase medium/total internalized]*100%).

Table 1

Internalization Mechanisms of MAP Peptides

Oligopeptide	% V[a]	ng/mL V	% C[a]	ng/mL C
^{125}I-MAP (n=12)	112 (16)[b]	545 (159)	ND[c]	ND[c]
^{125}I-gnd[d]-MAP (n=6)	35(9)	19(6)	65(9)	34(6)

[a] Percentage of total internalization measured in vesicles (V) and in the cytosol (C)

[b] Data are represented as the average of replicate measurements with standard deviations indicated in parentheses.

[c] ND = Not Detectable

[d] Gnd = Guanidinated epsilon-lysyl groups

Table 2

Nuclear Transport of CPPs[a]

CPP	CHO Cells		A431 Cells	
	Nuclear (nmol/mg nuclear protein)	Total Internalization (pmol/mg cell protein)	Nuclear (nmol/mg nuclear protein)	Total Internalization (pmol/mg cell protein)
MAP	1.4 (0.16)	120 (2.9)	1.3 (0.12)	121 (17.2)
$YG(R)_9$	0.89 (0.079)	18 (0.61)	0.20 (0.016)	20 (5.8)
TAT	0.48 (0.097)	13 (1.9)	0.15 (0.029)	21 (0.70)
$YG(K)_9$	0.084 (0.021)	8.6 (2.1)	0.086 (0.008)	12.5 (1.7)

[a]The data are represented as the average of replicate measurements (n > 3) with standard deviation shown in parenthesis.

[b]N/A: Data not available